First-principles study of Be doped $CuAlS_2$ for p-type transparent conductive materials

Dan Huang,[1,2,a)] Yu-Jun Zhao,[3,b)] Ren-Yu Tian,[3] Di-Hu Chen,[2] Jian-Jun Nie,[1] Xin-Hua Cai,[1] and Chun-Mei Yao[1]
[1]*Department of Physics and Electronic Sciences, Hunan University of Arts and Science, Changde, Hunan 415000, People's Republic of China*
[2]*School of Physics and Engineering, Sun Yat-sen University, Guangzhou 510275, People's Republic of China*
[3]*Department of Physics, South China University of Technology, Guangzhou 510640, People's Republic of China*

(Received 29 November 2010; accepted 9 March 2011; published online 7 June 2011)

$CuAlS_2$ has attracted much attention recently as a p-type transparent conductive material. In this paper, we investigate the site preference of substitutional Be in $CuAlS_2$ and the transition level of Be_{Al} using the first-principles calculation. We find that Be would be doped effectively at Al sites in $CuAlS_2$ as a good p-type dopant. In addition, we speculate that Be–Mg or Be–Zn codoped $CuAlS_2$ could have a mobility enhancement and thus a good p-type conductivity due to low lattice distortion. © *2011 American Institute of Physics*. [doi:10.1063/1.3574662]

I. INTRODUCTION

Transparent conductive materials (TCMs) belong to the class of wideband-gap semiconductors; by doping with shallow levels of impurities they can be made to possess the unique properties of the transparency of glass and the conductivity of metal. TCMs are widely and practically used as transparent electrodes in flat panel displays, solar cells, and touch panels. They usually possess carrier concentrations of at least 10^{20} cm^{-3}, optical band gaps greater than 3 eV, and conductivity greater than 1×10^4 S cm^{-1}.[1,2] Most of the industry standard TCMs are n-type, for example, Sn doped In_2O_3(ITO),[3] F doped SnO_2(FTO),[4] and Al doped ZnO (AZO).[5] Even so, the application of n-type TCMs is rather restricted without p-type TCMs because the active functions of most optoelectronic elements are based on p–n junctions. There is, however, still a lack of good p-type TCMs. The development of functional p–n junctions solely using TCMs is a vital goal for material scientists, because it is expected to open up an era of "transparent electronics."[2]

The first reports of p-type TCMs date back to 1997, when Kawazoe *et al.*[6] reported $CuAlO_2$ thin films. They reported that $CuAlO_2$ film possessed a conductivity of 1.0 S cm^{-1} at room temperature. After that, almost all copper-oxide-based delafossite structure semiconductors have been reported to be of p-type conductivity, such as $CuBO_2$,[7] $CuGaO_2$,[8] $CuInO_2$,[9] $CuScO_2$,[10] and $CuCrO_2$,[11] but their conductivities are 10^3 to 10^4 times lower than those of well-established n-type TCMs for the hole localization of oxides. Nie *et al.*[12] revealed that this delafossite family did not exhibit direct bandgap by first-principles study. This may impede the application of delafossite $CuM^{III}O_2$ because TCMs with a direct bandgap are preferred for the p–n junctions.[13]

Recently, a series of nonstoichiometric and Zn/Mg doped $CuAlS_2$ (Refs. 14–19) with chalcopyrite structures and direct bandgaps have been reported with significant promotions of high p-type conductivity at room temperature by experiment. For example, $CuAl_{0.9}Zn_{0.1}S_2$ (Ref. 18) has shown a conductivity of up to 63.5 S cm^{-1}, and the average transmittance in the visible region is above 80%. Yang *et al.*[19] have successfully prepared transparent p–n junctions with $CuAl_{1-x}Zn_xS_2$. From a theoretical point of view, we have studied the intrinsic defect and extrinsic Mg/Zn dopant in $CuAlS_2$,[20] indicating that Zn_{Al} could have a lower formation energy under favorable conditions. Our calculated transition level of Zn_{Al} is 0.14 eV, in accordance with good p-type conductivity found by experiment. We also find that the increased hole concentration in $Cu_{1-x}AlS_2$ is impeded mainly by the antisite defect Al_{Cu}. Even with a high hole concentration, it is found that the hole mobility of $CuAlS_2$ is hindered by the carrier's low mean free time,[20] in association with lattice distortion in general.

In this paper, using the first-principles calculation, we calculate the defect formation energy and transition level of Be_{Al} in Be doped $CuAlS_2$. In the most favorable chemical potential condition, the defect formation energy is about 0.55 eV for p-type samples in which Be is substituted for Al (i.e., the Fermi level is close to the valence-band maximum [VBM]). The transition level of Be_{Al} is 0.17 eV, indicating that Be should be a good dopant in $CuAlS_2$ for p-type conductive doping. In particular, we infer that Be–Zn or Be–Mg codoping would enhance mobility because Be–Zn or Be–Mg codoping decreases lattice distortion effectively.

II. COMPUTATIONAL DETAILS

Our first-principles calculations have been carried out using density functional theory (DFT) as implemented in the Vienna *ab initio* simulation package (VASP).[21,22] The Perdew-Burke-Ernzerhof gradient corrected function[23] is used with corrections for on-site Coulomb interactions for strongly correlated systems. Generalized gradients approximation (GGA) typically underbinds localized orbitals of 3*d*

[a)]Author to whom correspondence should be addressed. Electronic mail: danhuangdan@gmail.com.
[b)]Electronic mail: zhaoyj@scut.edu.cn.

Author complimentary copy. Redistribution subject to AIP license or copyright, see http://jap.aip.org/jap/copyright.jsp

transition metals, and the $+U$ modification provides an approximate correction for this shortcoming. The value of U_{eff} employed for the Cu d states is 5.2 eV, which is consistent with values determined by previous studies.[24,25] To describe the interactions between the valence electrons and the core, the projector augmented wave implementation[26] was used. For the $CuAlS_2$ unit cell, an energy cutoff of 700 eV and special K-point sampling over an $8 \times 8 \times 4$ Monkhorst–Pack mesh[27] were used. This ensured that the enthalpy differences converged to less than 0.03 meV/atom.

$CuAlS_2$ has a chalcopyrite structure (space group number: 122), which is analogous to a zinc-blende structure with its cations substituted by two types of cations alternatively along the $\langle 001 \rangle$ direction. Our calculated lattice parameters and the anion displacement parameter of $CuAlS_2$ are $a = b = 5.366$ Å, $c = 10.497$ Å, and $u = 0.259$, which are in good agreement with the experimental measurements $a = b = 5.334$ Å, $c = 10.444$ Å,[28] and $u = 0.268$.[29] For the formation energy calculation, $2 \times 2 \times 1$ supercells containing 64 atoms are used. For the doped supercells, the lattice constants are fixed as the optimized ideal lattice and other internal coordinates are fully relaxed throughout this work. The energy cutoff is set to 700 eV, while a K mesh of $4 \times 4 \times 6$ is employed for the $2 \times 2 \times 1$ supercells.

III. RESULTS AND DISCUSSION

Figure 1 shows the bandgap and partial density of states (PDOS) of $CuAlS_2$. $CuAlS_2$ is a direct bandgap semiconductor with a VBM and a conduction-band minimum (CBM) at the Γ point in the Brillouin zone. The underestimation of bandgaps is a well-known drawback of standard DFT calculations. Here, our GGA+U calculated bandgap, 2.29 eV, was still less than the experimental value, 3.49 eV. As shown from the PDOS, the majority of the upper valence band (−2 to 0 eV) is dominated by Cu $3d$ with a noticeable contribution from S $3p$. The atomic orbital level of Cu $3d$ is higher than that of O $2p$, which dominates the upper valence band of ZnO, SnO_2, In_2O_3, etc. This is attributed to the delocalization of the holes, which results in shallower, less localized acceptor levels above the valence band. The lower conduction band consists of Cu $3d$, S $4s$, S $4p$, and S $3d$. At the VBM, the calculated hole effective masses are $m_{100} = m_{010} = 2.519$ m_e and $m_{001} = 0.681$ m_e without spin-orbit coupling in the [100], [010], and [001] directions, respectively. When the spin-orbit coupling is considered, the effective masses change to $m^{SO}{}_{100} = m^{SO}{}_{010} = 2.989$ m_e and $m^{SO}{}_{001} = 0.643$ m_e, respectively. This indicates that the spin-orbit coupling has no significant influence on the lightest effective mass in the [001] direction, although the values in the other two directions increase remarkably. The hole effective mass in the [001] direction has the same order as that of the good n-type TCMs In_2O_3, 0.24 m_e.[30]

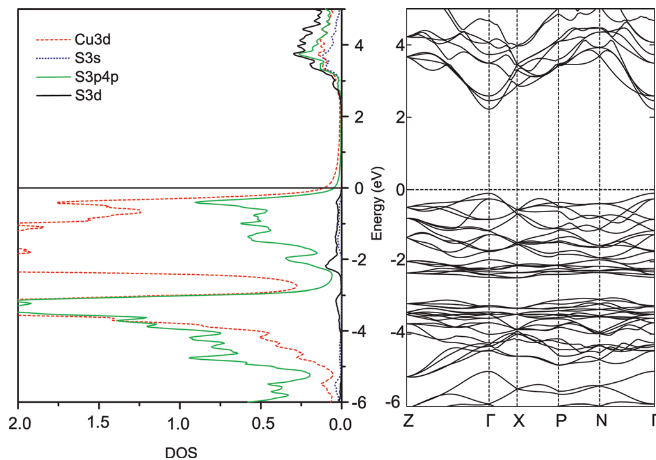

FIG. 1. (Color online) The bandgap and partial density of states of $CuAlS_2$.

Next, we investigate the site preference of Be at Cu or Al sites. The site preference is crucial to the electronic property of the sample because Be defects are expected to be donors at Cu sites but acceptors at Al sites. Their favorable doping site can be determined by their defect formation enthalpies, which depend on the growth conditions.

The formation enthalpies for the Be doping at Cu or Al sites are calculated in a $2 \times 2 \times 1$ $CuAlS_2$ supercell consisting of 64 atoms according to[31]

$$\Delta H(D,q) = E(D,q) - E(0) + \sum_{\alpha} n_{\alpha}(\Delta\mu_{\alpha} + \mu_{\alpha}^{\text{solid}}) + q(E_{\text{VBM}} + E_F), \quad (1)$$

where $E(D,q)$ and $E(0)$ are the total energy of the supercells with and without defect, respectively. Here $(\Delta\mu_{\alpha} + \mu_{\alpha}^{\text{solid}})$ is the absolute value of the chemical potential of atom α. $\mu_{\alpha}^{\text{solid}}$ is defined as the chemical potential of the elemental solid. Also, n_{α} is the number of atoms for each defect; $n_{\alpha} = -1$ if an atom is added, while $n_{\alpha} = 1$ if an atom is removed. E_{VBM} represents the energy of the VBM of the defect-free system, and E_F is the Fermi energy relative to the E_{VBM}. For charged systems, a compensating homogeneous jellium background charge is assumed to preserve overall neutrality. Recently, Lany and Zunger[32] found that the formation energy of GaAs:-V_{As}^{3+} could be well converged in fairly small supercells such as a 64-atom or even 32-atom supercell, as long as the potential alignment and image charge correction are included. Considering the 64-atom supercells adopted in this work, we have carried out the calculations with both the potential alignment and the image charge correction. The potential alignment is considered by adding ΔV into the $(E_{\text{VBM}} + E_F)$ term, where ΔV is the electrostatic alignment between the doped host and the pure host. The full third order image charge correction can be accurately approximated by a simple scaling factor (2/3) for the first order (screened) Madelung term, as suggested by Lany and Zunger.[32]

The chemical potentials of each constituent species $(\Delta\mu_{\alpha})$ can be varied to reflect specific equilibrium growth conditions, but their summation is always equal to the calculated formation enthalpy of $CuAlS_2$ in order to maintain the stability of the host:

$$\Delta\mu_{\text{Cu}} + \Delta\mu_{\text{Al}} + 2\Delta\mu_{\text{S}} = \Delta H(\text{CuAlS}_2). \quad (2)$$

In addition to the host stability condition, the atomic chemical potentials should be smaller than that of the corresponding

Author complimentary copy. Redistribution subject to AIP license or copyright, see http://jap.aip.org/jap/copyright.jsp

TABLE I. The crystal structure and the calculated and experimental enthalpy of all related compounds.

	Crystal structure	Calculated enthalpy (eV)	Experimental enthalpy (eV)
$CuAlS_2$	Tetragonal Space group number: 122	−3.500	
Al_2S_3	Hexagonal Space group number: 169	−5.267	−7.504[a]
$CuAl_5S_8$	Cubic Space group number: 227	−14.167	
Cu_2S	Tetragonal Space group number: 96	−0.738	−0.824[a]
CuS	Hexagonal Space group number: 194	−0.506	−0.550[a]
BeS	Cubic Space group number: 216	−2.121	−2.428[a]

[a]Reference 34.

elemental solid in order to avoid precipitation of elemental solids:

$$\Delta\mu_{Cu} \leq 0,\ \Delta\mu_{Al} \leq 0,\ \Delta\mu_S \leq 0. \quad (3)$$

The chemical potentials are further restricted by the competing compounds. Referring to our previous works,[20,33] these crucial constraints are listed as the following:

$$2\Delta\mu_{Al} + 3\Delta\mu_S \leq \Delta H(Al_2S_3), \quad (4)$$

$$\Delta\mu_{Cu} + \Delta\mu_S \leq \Delta H(CuS), \quad (5)$$

$$2\Delta\mu_{Cu} + \Delta\mu_S \leq \Delta H(Cu_2S), \quad (6)$$

$$\Delta\mu_{Cu} + 5\Delta\mu_{Al} + 8\Delta\mu_S \leq \Delta H(CuAl_5S_8). \quad (7)$$

Table I lists the enthalpies of all of the related compounds. We found that the GGA+U calculated enthalpies of CuS and Cu_2S were in better agreement with the corresponding experimental values as compared with our previous GGA results.[20,33] Under the constraints imposed by the competing compounds, the shaded areas in Fig. 2 are the allowed chemical potential ranges for $CuAlS_2$. Assuming a Fermi energy level at 0.15 eV above the VBM,[20] the formation enthalpy of Be_{Al} would be smaller/bigger than that of Be_{Cu} in the green/yellow (lower/upper gray in black/white) area. If the Fermi energy level moves toward the CBM, Be_{Al} preference in the ($\Delta\mu_{Cu}$, $\Delta\mu_{Al}$) plane would increase. A balance point for the Fermi level must exist because Be_{Al} is an acceptor, which would impede the Fermi energy level's movement toward the CBM. In order to get p-type TCMs by doping with Be, we intend to dope with Be at Al sites rather than Cu sites as much as possible. Therefore, point M is chosen as the optimal growth condition. To have the lowest formation enthalpy of Be_{Al}, we expect that $\Delta\mu_{Be}$ could reach the maximum value. When Be is introduced into the $CuAlS_2$ systems, however, the chemical domain of $CuAlS_2$ may be further limited due to the competing phases of BeS, with a constraint of

$$\Delta\mu_{Be} + \Delta\mu_S \leq \Delta H(BeS). \quad (8)$$

Because ΔH(BeS) is a constant, the maximum allowed chemical potential for Be is directly dependent on $\Delta\mu_S$. At point M, the maximum allowed value of $\Delta\mu_{Be}$ is -1.85 eV (red (dark gray in black/white) line in Fig. 2).

Figure 3 shows the formation enthalpy of Be_{Al} and Be_{Cu} under maximum values of point M and $\Delta\mu_{Be}$. If the Fermi energy level is at 0.15 eV above the VBM, the formation enthalpy of Be_{Al} should be 0.55 eV. The transition level of Be_{Al} is calculated to be 0.17 eV, indicating that Be could be doped at Al sites effectively as a shallow impurity-level dopant and could improve p-type carrier concentration. In reality, the final electrical conductivity σ ($\sigma = pq\mu_p$) depends on not only the carrier concentration p, but also the hole mobility μ_p($\mu_p = q\tau_p/m^*$). Our former study[20] showed that the difference in the effective mass is negligible between the carriers originating from various defects. Recently, Mao *et al.*[35] found that there was a great mobility enhancement

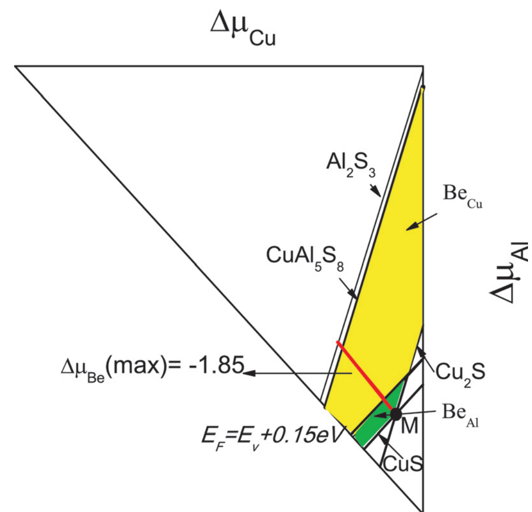

FIG. 2. (Color online) The GGA+U calculated chemical potential range for site preference on Cu or Al of the dopant atom Be (assuming $E_F = 0.15$ eV for Be doping). The yellow (upper gray in black/white) area favors the Cu site, while the green (lower gray in black/white) area favors the Al site for the dopants.

Author complimentary copy. Redistribution subject to AIP license or copyright, see http://jap.aip.org/jap/copyright.jsp

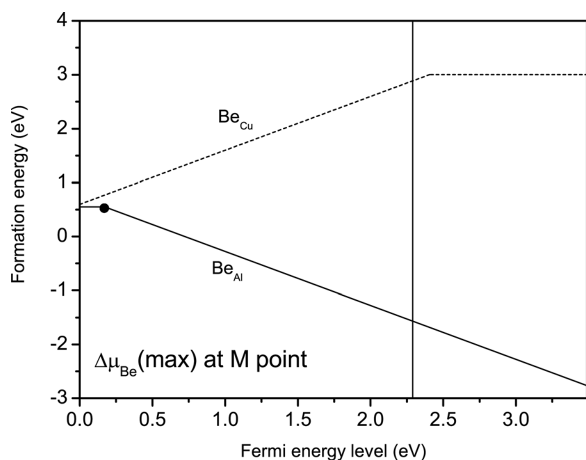

FIG. 3. The formation enthalpy of Be ($\Delta\mu_{Be} = -1.85$ eV) doped in $CuAlS_2$ under point M in Fig. 2. The vertical line is our calculated bandgap. Solid lines and dashed lines represent the acceptor and donor defects, respectively. Here the experimental gap of $CuAlS_2$, $E_g = 3.49$ eV, is adopted.

(10^3 to 10^4 times) with In–Ga codoping in SnO_2 compared with In or Ga doping. Owing to the ion radius following the sequence of $Ga^{3+} < Sn^{4+} < In^{3+}$, In–Ga codoping is expected to decrease SnO_2 lattice distortion effectively compared to In doped and Ga doped SnO_2. This shows that the lattice distortion has an important effect on the mobility. In our calculation, the bond length of $Be_{Al}{}^0$–S is 2.15 Å, which is shorter than the bond length of Al–S (2.28 Å). Meanwhile, we investigated the Mg and Zn (GGA+U on Zn 3d with the U value from Ref. 36) doped $CuAlS_2$. The bond lengths of $Mg_{Al}{}^0$–S and $Zn_{Al}{}^0$–S are 2.41 Å and 2.34 Å, respectively, which are both longer than that of Al–S. Therefore, Be–Mg or Be–Zn doped $CuAlS_2$ would have a weaker lattice distortion than the Be, Mg, or Zn doped $CuAlS_2$. We therefore speculate that Be–Mg or Be–Zn codoped $CuAlS_2$ could have enhanced mobility, as well as a better p-type conductivity, because they are both shallow impurities.

IV. CONCLUSION

In summary, we have calculated the formation energies and transition levels of Be-related defects in $CuAlS_2$ by using the first-principles calculations. We find that the formation energy of Be_{Al} is about 0.55 eV at the most favorable condition in p-type samples, and its transition level is 0.17 eV. Therefore, Be could be doped at Al sites effectively in $CuAlS_2$ as a good p-type dopant. Furthermore, Be–Mg or Be–Zn codoped $CuAlS_2$ is expected to have enhanced mobility and a good p-type conductivity because Be–Mg and Be–Zn codoping reduces the lattice distortion with respect to $CuAlS_2$:Zn and $CuAlS_2$:Mg.

ACKNOWLEDGMENTS

This work was financially supported by the National Natural Science Foundation of China (NSFC) under Grant No. 10704025; the Fundamental Research Funds for the Central Universities, SCUT, under projects 2009ZZ0068 and 2009ZM0165; the Key Construction Academic Subject (Optics) of Hunan Province; and the Natural Science Foundation of Hunan Province (09JJ3004). The authors acknowledge computer time at the High Performance Computer Center of the Shenzhen Institute of Advanced Technology (SIAT), the Chinese Academy of Science.

[1]R. G. Gordon, MRS Bull. **25**, 52 (2000).
[2]G. Thomas, Nature **389**, 907 (1997).
[3]S. P. Harvey, T. O. Mason, Y. Gassenbauer, R. Schafranek, and A. Klein, J. Phys. D: Appl. Phys. **39**, 3959 (2006).
[4]Z. Remes, M. Vanecek, H. M. Yates, P. Evans, and D.W. Sheel, Thin Solid Films **517**, 6287 (2009).
[5]K. Y. Wu, C. C. Wang, and D. H. Chen, Nanotechnology **18**, 305604 (2007).
[6]H. Kawazoe, M. Yasukawa, H. Hyodo, M. Kurita, H. Yanagi, and H. Hosono, Nature **389**, 939 (1997).
[7]M. Snure and A. Tiwari, Appl. Phys. Lett. **91**, 092123 (2007).
[8]K. Ueda, T. Hase, H. Yanagi, H. Kawazoe, H. Hosono, H. Ohta, M. Orita, and M. Hirano, J. Appl. Phys. **89**, 1790 (2001).
[9]C. W. Teplin, T. Kaydanova, D. L. Young, J. D. Perkins, D. S. Ginley, A. Ode, and D. W. Readey, Appl. Phys. Lett. **85**, 3789 (2004).
[10]N. Duan, A. W. Sleight, M. K. Jayaraj, and J. Tate, Appl. Phys. Lett. **77**, 1325 (2000).
[11]R. Nagarajan, A. D. Draeseke, A. W. Sleight, and J. Tate, J. Appl. Phys. **89**, 8022 (2001).
[12]X. L. Nie, S. H. Wei, and S. B. Zhang, Phys. Rev. Lett. **88**, 066405 (2002).
[13]K. G. Godinho, J. J. Carey, B. J. Morgan, D. O. Scanlon, and G. W. Watson, J. Mater. Chem. **20**, 1086 (2010).
[14]M. L. Liu, F. Q. Huang, and L. D. Chen, Key Eng. Mater. **368–372**, 666 (2008).
[15]F. Q. Huang, M. L. Liu, L. B. Wu, and L. D. Chen, China patent No. 200610025073.1 (2006).
[16]M. L. Liu, Y. M. Wang, F. Q. Huang, L. D. Chen, and W. D. Wang, Scr. Mater. **57**, 1133 (2007).
[17]M. L. Liu, F. Q. Huang, and L. D. Chen, Scr. Mater. **58**, 1002 (2008).
[18]M. L. Liu, F. Q. Huang, L. D. Chen, Y. M. Wang, Y. H. Wang, G. F. Li, and Q. Zhang, Appl. Phys. Lett. **90**, 072109 (2007).
[19]M. Yang, Y. H. Wang, G. F. Li, Z. Shi, and Q. Zhang, J. Vac. Sci. Technol. A **27**, 1316 (2009).
[20]D. Huang, R. Y. Tian, Y. J. Zhao, J. J. Nie, X. H. Cai, and C. M. Yao, J. Phys. D: Appl. Phys. **43**, 395405 (2010).
[21]G. Kresse and J. Hafner, Phys. Rev. B **47**, 558 (1993).
[22]G. Kresse and J. Furthmüller, Phys. Rev. B **54**, 11169 (1996).
[23]J. P. Perdew, K. Burke, and M. Ernzerhof, Phys. Rev. Lett. **77**, 3865 (1996).
[24]D. O. Scanlon, K. G. Godinho, B. J. Morgan, and G. W. Watson, J. Chem. Phys. **132**, 024707 (2010).
[25]D. O. Scanlon, A. Walsh, B. J. Morgan, and G. W. Watson, Phys. Rev. B **79**, 035101 (2009).
[26]G. Kresse and J. Joubert, Phys. Rev. B **59**, 1758 (1999).
[27]H. J. Monkhorst and J. D. Pack, Phys. Rev. B **13**, 5188 (1976).
[28]G. Brandt, A. Rauber, and J. Schneider, Solid State Commun. **12**, 481 (1973).
[29]W. Zalewski, R. Bacewicz, J. Antonowicz, S. Schorr, C. Streeck, and B. Korzun, Phys. Status Solidi A **205**, 2428 (2008).
[30]A. Walsh, J. L. F. Da Silva, and S. H. Wei, Phys. Rev. B **78**, 075211 (2008).
[31]S. B. Zhang, S. H. Wei, and A. Zunger, Phys. Rev. B **63**, 075205 (2001).
[32]S. Lany and A. Zunger, Phys. Rev. B **78**, 235104 (2008).
[33]Y. J. Zhao and A. Zunger, Phys. Rev. B **69**, 075208 (2004).
[34]*CRC Handbook of Chemistry and Physics*, 88th ed., edited by D. R. Lide (CRC Press/Taylor & Francis, Boca Raton, FL, 2007).
[35]Q. N. Mao, Z. G. Ji, and L. N. Zhao, Phys. Status Solidi B **247**, 299 (2010).
[36]A. Schleife, C. Rödl, F. Fuchs, J. Furthmüller, and F. Bechstedt, Phys. Rev. B **80**, 035112 (2009).

Author complimentary copy. Redistribution subject to AIP license or copyright, see http://jap.aip.org/jap/copyright.jsp